Computing the roughening transition of Ising and solid-on-solid models by BCSOS model matching

1997 J. Phys. A: Math. Gen. 30 63

(http://iopscience.iop.org/0305-4470/30/1/006)

J. Phys. A: Math. Gen. **30** (1997) 63–80. Printed in the UK PII: S0305-4470(97)74429-9

Computing the roughening transition of Ising and solid-on-solid models by BCSOS model matching

M Hasenbusch†§ and K Pinn‡‖

† Fachbereich Physik, Humboldt Universität zu Berlin, Invalidenstrasse 110, 10099 Berlin, Germany

‡ Institut für Theoretische Physik I, Universität Münster, Wilhelm-Klemm-Strasse 9, D-48149 Münster, Germany

Received 10 May 1996, in final form 18 September 1996

Abstract. We study the roughening transition of the dual of the two-dimensional (2D) XY model, of the discrete Gaussian model, of the absolute value solid-on-solid model and of the interface in an Ising model on a three-dimensional (3D) simple cubic lattice. The investigation relies on a renormalization group finite size scaling method that was proposed and successfully tested a few years ago. The basic idea is to match the renormalization group flow of the interface observables with that of the exactly solvable body-centred solid-on-solid (BCSOS) model. Our estimates for the critical couplings are $\beta_{\rm R}^{\rm XY} = 1.1199(1)$, $K_{\rm R}^{\rm DG} = 0.6653(2)$ and $K_{\rm R}^{\rm ASOS} = 0.806\,08(2)$ for the XY model, the discrete Gaussian model and the absolute value solid-on-solid model, respectively. For the inverse roughening temperature of the Ising interface we find $K_{\rm R}^{\rm Ising} = 0.407\,58(1)$. To the best of our knowledge, these are the most precise estimates for these parameters published so far.

1. Introduction

Among the phase transitions that occur in 2D or effectively 2D statistical systems, those of the so-called Kosterlitz–Thouless (KT) type [1] belong to the most challenging. The KT phase transition is of infinite order: the free energy and all its derivatives stay finite at the transition point. Despite the relatively simple arguments that suggest the existence of such a transition in a variety of systems, a rigorous proof of the KT nature of the phase transition in many physically interesting systems is still lacking. Also all of the numerical studies (many of them Monte Carlo studies of the 2D XY model) could not provide an unambigious confirmation of the KT scenario. A number of references will be given in section 5.

The reason for the problem is the appearance of corrections to scaling that vanish only logarithmically with the system size. Most of the investigations based on simulations of KT models on finite lattices suffer from these corrections.

Note, however, that there exists at least one 2D lattice model, which has been *proven* to undergo a KT transition by exact solution. This is the body-centred solid-on-solid (BCSOS) model [2], the configurations of which are, up to boundary conditions, in one-to-one correspondence with those of a special six-vertex model [3–5], the F-model.

A few years ago we proposed a method that allows one to investigate the KT transition of a given model by comparing its block spin renormalization group (RG) flow (on finite

§ E-mail address: hasenbus@birke.physik.hu-berlin.de
‖ E-mail address: pinn@uni-muenster.de

0305-4470/97/010063+18$19.50

lattices) with that of the BCSOS model [6, 7]. A matching of the two RG flows at long distance (large blocks) demonstrates that the models belong to the same universality class, which is the KT class here.

In contrast to the usual approaches, the method introduces systematic errors that decay like L^{-2}, where L is the size of the lattices involved in the computations.

Our approach has been successfully applied to the absolute-value solid-on-solid (ASOS) model, the discrete Gaussian (DG) model and the dual of the standard XY model in two dimensions [6]. Successful applications to the interface of the Ising model were performed in [7], and, recently, in [8].

In the present paper we improve on the results of [6] by using larger lattice sizes and increasing the statistics by a factor of about 100. This became affordable both by the availability of faster computers and the use of more efficient program code.

This paper is organized as follows. In section 2 we define the models and state the exact results for the BCSOS model relevant to our study. We briefly discuss the KT flow equations. Section 3 is devoted to a description of the matching method. In section 4 we present and discuss our numerical results. A comparison with previous estimates of the critical couplings and non-universal parameters is presented in section 5. Conclusions and an outlook follow.

2. Ising model interfaces and solid-on-solid models

2.1. Ising model interfaces

We consider the 3D Ising model on the simple cubic lattice, with Hamiltonian

$$H = -\sum_{\langle x,y\rangle} s_x s_y \qquad s_x = \pm 1. \tag{1}$$

The sites of the lattice are labelled by integer coordinates $x = (x_1, x_2, x_3)$. The sum in equation (1) is over all (unordered) nearest-neighbour pairs of sites in the lattice. The partition function is

$$Z = \sum_{\{s\}} \exp(-K^{\mathrm{I}} H). \tag{2}$$

Here, the summation is over all possible configurations of the Ising spins. The pair interaction is normalized such that $K^{\mathrm{I}} = 1/(k_{\mathrm{B}}T)$, where k_{B} denotes Boltzmann's constant, and T is the temperature.

At a critical coupling $K^{\mathrm{I}}_{\mathrm{c}}$ (the estimate of a recent study [9] is $K^{\mathrm{I}}_{\mathrm{c}} = 0.221\,6546(10)$) the infinite volume limit of the model undergoes a second-order phase transition. For $K^{\mathrm{I}} > K^{\mathrm{I}}_{\mathrm{c}}$, the system shows spontaneous breaking of the reflection symmetry.

In order to study interfaces separating extended domains of different magnetization, we consider lattices with extension L in the x_1- and x_2-directions and with extension D in the x_3-direction. We generalize equation (1) to

$$H = -\sum_{\langle x,y\rangle} k_{xy} s_x s_y. \tag{3}$$

The lattice becomes a torus by regarding the opposite boundary planes as neighbour planes. For the Ising spins s we will apply antiperiodic boundary conditions in the x_3-direction, by letting $k_{xy} = -1$ for the links that connect the uppermost with the lowermost plane. For the other links we set $k_{xy} = 1$.

For sufficiently large K^{I} and large enough L, the imposure of antiperiodic boundary conditions forces the system to develop exactly one interface, which is a region where the magnetization rapidly changes sign. This interface is parallel to a (001) lattice plane.

The Ising (001) interface undergoes a *roughening transition* at an inverse temperature $K_{\mathrm{R}}^{\mathrm{I}} = 1/(k_{\mathrm{B}}T_{\mathrm{R}})$ that is nearly twice as large as the bulk transition coupling $K_{\mathrm{c}}^{\mathrm{I}}$ given above†. In this work, we shall determine a new estimate for $K_{\mathrm{R}}^{\mathrm{I}}$, and also for other parameters of the roughening transition. For a collection of previous estimates, see section 5.

At the roughening transition, the large scale interface behaviour changes from being rigid or smooth at low temperature to being rough at high temperature. The transition shows up in a characteristic behaviour of various quantities. For example, in the smooth phase, the interfacial width stays finite when L tends to infinity, while it diverges logarithmically with the system size in the rough phase [11, 12]. For general introductions to roughening, see [13–15]. For comparisons of real life experiments with theory see, for example [16].

2.2. Solid-on-solid models

A fairly good approximation of the Ising interface is given by the solid-on-solid (SOS) models to be introduced in this section. The SOS approximation amounts to ignoring overhangs of the Ising interface and bubbles in the two phases separated by the interface. For a review of exact results on SOS types of models, see, for example [13]. By duality [17] and other exact transformations (see, e.g. [18]), SOS models have been shown to be equivalent to a variety of other statistical models.

All SOS models that we shall consider have in common that they are 2D lattice spin models.

Our first example of an SOS model is the ASOS model. It can be considered as the SOS approximation of an (001) lattice plane interface of an Ising model on a simple cubic lattice. The model is defined by the Hamiltonian

$$H_{\mathrm{ASOS}} = K^{\mathrm{ASOS}}|h_x - h_y|. \tag{4}$$

The spin variables h_x take integer values. Here and in the following, the Boltzmannian will always be $\exp(-H)$. A factor $1/(k_{\mathrm{B}}T)$, where k_{B} denotes Boltzmann's constant and T the temperature, is absorbed in the definition of the Hamiltonian.

We interpret the h_x as heights with respect to a certain base. For finite positive K^{ASOS} the Hamiltonian will favour that neighbouring spins take similar values. When K^{ASOS} is large enough, the surface will not fluctuate too wildly (smooth phase). On the other hand, if K^{ASOS} is below a certain critical value, the surface becomes 'rough', and, for example, the surface thickness diverges when the system size goes to infinity.

Let us now turn to the discrete Gaussian (DG) model. The Hamiltonian is

$$H_{\mathrm{DG}} = K^{\mathrm{DG}}(h_x - h_y)^2. \tag{5}$$

The spin variables h_x take integer values. Note that the Hamiltonian looks exactly like that of a continuous Gaussian model. However, the restriction of the h_x to integer values introduces a non-trivial interaction. The discrete Gaussian model is dual to the XY model with Villain action [17]‡. This model is defined by the partition function

$$Z_V = \int_{-\pi}^{\pi} \prod_x \mathrm{d}\Theta_x \prod_{\langle x,y\rangle} B(\Theta_x - \Theta_y) \tag{6}$$

† A pioneering work on this issue is [10].

‡ What is called Hamiltonian in the language of statistical mechanics is called action in the framework of Euclidean quantum field theory.

with

$$B(\Theta) = \sum_{p=-\infty}^{\infty} \exp(-\tfrac{1}{2}\beta_{\mathrm{V}}(\Theta - 2\pi p)^2) \tag{7}$$

and

$$\frac{1}{2\beta_{\mathrm{V}}} = K^{\mathrm{DG}}. \tag{8}$$

The index 'V' here refers to 'Villain'.

The XY model with 'standard (cosine) action' has the partition function

$$Z_{\mathrm{XY}} = \int_{-\pi}^{\pi} \prod_x \mathrm{d}\Theta_x \exp\left(\beta^{\mathrm{XY}} \sum_{\langle x,y\rangle} \cos(\Theta_x - \Theta_y)\right). \tag{9}$$

The standard action is the mostly discussed action for an XY model. The dual of this model is given by the partition function

$$Z_{\mathrm{XY}}^{\mathrm{SOS}} = \sum_{\{h\}} \prod_{\langle x,y\rangle} I_{|h_x - h_y|}(\beta^{\mathrm{XY}}) \tag{10}$$

where the I_n are modified Bessel functions. Again h_x is integer.

We finally introduce the BCSOS or F-model. The BCSOS model was introduced by van Beijeren [2] as an SOS approximation of an interface in an Ising model on a body-centred cubic lattice on a (001) lattice plane. For a detailed analysis of this model with respect to roughening and surface structure, see [14, 15, 19]. The effective 2D lattice splits in two sublattices like a checker board. In the original formulation, on one of the sublattices the spins take integer values, whereas the spins on the other sublattice take half-integer values. We adopt a different convention: spins on 'odd' lattice sites take values of the form $2n + \frac{1}{2}$, and spins on 'even' sites are of the form $2n - \frac{1}{2}$, n integer. The Hamiltonian of the BCSOS model can be expressed as

$$H_{\mathrm{BCSOS}} = K^{\mathrm{BCSOS}} \sum_{[x,y]} |h_x - h_y|. \tag{11}$$

The sum is over next-to-nearest-neighbour pairs $[x, y]$, and nearest-neighbour spins h_x and h_y obey the constraint $|h_x - h_y| = 1$. Van Beijeren [2] showed that the BCSOS model can be transformed into the F-model, which is a special six-vertex model. The F-model can be solved exactly with transfer matrix methods [3–5]. The roughening transition occurs at

$$K_{\mathrm{R}}^{\mathrm{BCSOS}} = \tfrac{1}{2}\ln 2. \tag{12}$$

For $K \searrow K_{\mathrm{R}}$, the correlation length behaves like

$$\xi^{\mathrm{BCSOS}} \simeq \frac{1}{4}\exp\left(\frac{\pi^2}{8\sqrt{\frac{1}{2}\ln 2}}\kappa^{-\frac{1}{2}}\right) \qquad \kappa = \frac{K - K_{\mathrm{R}}}{K_{\mathrm{R}}}. \tag{13}$$

2.3. Renormalization group flow of interface models

It is believed (though not proven rigorously) that, in the vicinity of the fixed point relevant for the KT transition, the RG flow of SOS models and also of the 3D Ising model interface is well described by two parameters β and z [1]. The two parameters are the inverse temperature and a fugacity z.

The 2D sine–Gordon model is especially suited to discuss the flow of these parameters with the length scale, since this model contains β and z as bare parameters in its Hamiltonian:

$$H^{\mathrm{SG}} = \frac{1}{2\beta}\sum_{\langle x,y\rangle}(\phi_x - \phi_y)^2 - z\sum_x \cos(2\pi\phi_x) \tag{14}$$

where the ϕ_x are real numbers. For the continuum version of the model, with a momentum cut-off, one can derive the parameter flow under infinitesimal RG transformations [1]. It is given by

$$\dot{\boldsymbol{x}} = -\boldsymbol{z}^2 \qquad \dot{\boldsymbol{z}} = -\boldsymbol{x}\boldsymbol{z} \tag{15}$$

where $\boldsymbol{z} = \text{constant} \cdot z$ and $\boldsymbol{x} = \pi\beta - 2$. The constant depends on the particular cut-off scheme used. The derivative is taken with respect to the logarithm of the cut-off scale.

For large $\boldsymbol{x}$ the fugacity $\boldsymbol{z}$ flows towards $\boldsymbol{z} = 0$. The large distance behaviour of the model is therefore that of a Gaussian model (without a mass term). For small $\boldsymbol{x}$, $\boldsymbol{z}$ grows with increasing length scale. The theory is therefore massive, i.e. has finite correlation length. The critical trajectory separates these two regions in the coupling constant space. It ends at a Gaussian fixed point characterized by $\boldsymbol{x} = 0$ or $\beta = 2/\pi$. On the critical trajectory the fugacity vanishes as

$$\boldsymbol{z}(t) = \frac{1}{\boldsymbol{z}_0^{-1} + t} \tag{16}$$

where t is the logarithm of the cut-off scale. Equations (15) are the basis for KT theory. Its immediate consequences are derived in statistical mechanics text books, see for example [20]. For instance, the correlation length in the smooth phase of an SOS model should diverge like

$$\xi \simeq A\exp(C\kappa^{-1/2}) \qquad \kappa = \frac{K - K_{\mathrm{R}}}{K_{\mathrm{R}}} \tag{17}$$

when $K \to K_{\mathrm{R}}$. Note that this behaviour is precisely the one found for the BCSOS model by exact solution (cf equation (13)).

We would like to emphasize another important consequence of the KT equations that becomes apparent from the solution equation (16): at criticality, the fugacity, which parametrizes the deviation of the theory from a massless Gaussian model, decays with increasing scale $t = \ln L$, only like $(\ln L)^{-1}$. In lattice studies, L is more or less the lattice extension. Therefore, any method that is based on an observation of the Gaussian behaviour at long distance, suffers strongly from finite fugacity corrections even on very large lattices.

3. The matching method

The method of [6] is closely related to the finite size scaling methods proposed by Nightingale [21] and Binder [22]. No attempt is made to compute the RG flow of the couplings explicitly, but rather the RG flow is monitored by evaluating quantities that are primarily sensitive to the lowest frequency fluctuations on a finite lattice. One should stress that the method does not use any of the quantitative results of KT theory. Merely the qualitative result that there are two important coupling parameters in the flow is used.

In order to separate the low-frequency modes of the field a block spin transformation [23, 24] is used. Blocked systems of size $l \times l$ are considered. The size B of a block

(measured in units of the original lattice spacing) is then given by $B = L/l$, where L is the linear size of the original lattice. The linear blocking procedure defined by

$$\phi_X = B^{-2} \sum_{x \in X} h_x \tag{18}$$

where X labels square blocks of a linear extension B, is used. This linear blocking rule has the half-group property that the successive application of two transformations with a scale factor of B have exactly the same effect as a single transformation with a scale factor of B^2.

Motivated by the perturbation theory of the sine–Gordon model, two types of observables are chosen: those that are 'sensitive' to the flow of the kinetic term (flow of K), and those that are sensitive to the fugacity (periodic perturbation of a massless Gaussian model). For the first type of observables

$$A_1 = \langle (\phi_X - \phi_Y)^2 \rangle \tag{19}$$

where X and Y are nearest neighbours on the block lattice, and

$$A_2 = \langle (\phi_X - \phi_Z)^2 \rangle \tag{20}$$

where X and Z are next-to-nearest neighbours, are chosen. Note that these quantities are only defined for $l > 1$. As a monitor for the fugacity the following set of quantities (defined for $l = 1, 2, 4$ and 8) is taken:

$$A_3 = \langle \cos(1 \cdot 2\pi\phi_X) \rangle \qquad A_4 = \langle \cos(2 \cdot 2\pi\phi_X) \rangle. \tag{21}$$

3.1. Determination of the roughening coupling

There are two parameters which have to be adjusted in order to match the RG flow of an SOS model or of the Ising interface with that of the critical BCSOS model: the coupling K^{S} of the solid-on-solid or Ising model and in addition the ratio $b = B^{\mathrm{S}}/B^{\mathrm{B}} = L^{\mathrm{S}}/L^{\mathrm{B}}$ of the lattice sizes (and hence the block sizes) of the SOS or Ising model and the BCSOS model. In general a $b \neq 1$ is necessary to compensate for the different starting points of the two models on the critical RG trajectory [6]. For the proper values of the roughening coupling $K_{\mathrm{R}}^{\mathrm{S}}$ and the matching constant b observables of the SOS and the BCSOS model match like

$$A_{i,l}^{\mathrm{S}}(b\ B, K_{\mathrm{R}}^{\mathrm{S}}) = A_{i,l}^{\mathrm{B}}(B, K_{\mathrm{R}}^{\mathrm{B}}) + \mathrm{O}(B^{-\omega}) \tag{22}$$

where i labels the observable and l the size of the blocked lattice. The $\mathrm{O}(B^{-\omega})$ corrections are due to irrelevant operators. ω is the correction to the scaling exponent. The perturbation theory of the sine–Gordon model suggests $\omega = 2$.

In order to obtain numerical estimates for the roughening coupling $K_{\mathrm{R}}^{\mathrm{S}}$ and the matching factor b for a given lattice size L^{B} of the BCSOS model, we require that equation (22) is exactly fulfilled for two block observables.

We solve the system of two equations for the two observables $A_{i,l}$ and $A_{j,l}$ numerically by first computing the $K_{i,l}^{\mathrm{S}}(b)$ and $K_{j,l}^{\mathrm{S}}(b)$ that solve the single equations for a given value of b. The intersection of the two curves $K_{i,l}^{\mathrm{S}}(b)$ and $K_{j,l}^{\mathrm{S}}(b)$ gives us then the solution of the system of two equations. For an illustration of this method see figures 5 and 6 of [6].

In [6] we demonstrated that the corrections to scaling for the observables A_1 and A_2 for SOS models are similar to those in the massless continuous Gaussian model. Therefore we considered the 'improved' observable D_1 which is defined as follows:

$$D_1(L) = \frac{A_1^{(0)}(\infty)}{A_1^{(0)}(L)} A_1(L). \tag{23}$$

$A_1^{(0)}$ is computed for the massless Gaussian model defined by

$$H_0 = \frac{1}{2}\sum_{\langle x,y\rangle}(\psi_x - \psi_y)^2. \tag{24}$$

An improved quantity D_2 is defined analogously. Explicit results for $A_1^{(0)}$ and $A_2^{(0)}$ are given in table 1.

Table 1. Exact results for $A_1^{(0)}$ and $A_2^{(0)}$ as functions of the size of the fundamental lattice (L) and the size of the blocked lattice (l). The last row contains values extrapolated to $L = \infty$.

L	$A_{1,2}^{(0)}$	$A_{2,2}^{(0)}$	$A_{1,4}^{(0)}$	$A_{2,4}^{(0)}$	$A_{1,8}^{(0)}$	$A_{2,8}^{(0)}$
16	0.123 1474	0.171 8750	0.243 9180	0.326 0905	0.317 7271	0.423 0146
24	0.120 5651	0.168 9815	0.234 1466	0.315 6629	0.281 5115	0.383 4000
32	0.119 6545	0.167 9687	0.230 6619	0.311 9780	0.268 2336	0.369 1650
40	0.119 2317	0.167 5000	0.229 0354	0.310 2652	0.261 9443	0.362 4936
48	0.119 0016	0.167 2454	0.228 1480	0.309 3327	0.258 4828	0.358 8444
56	0.118 8628	0.167 0918	0.227 6114	0.308 7697	0.256 3784	0.356 6345
64	0.118 7726	0.166 9922	0.227 2625	0.308 4039	0.255 0051	0.355 1961
80	0.118 6664	0.166 8750	0.226 8516	0.307 9734	0.253 3820	0.353 5002
96	0.118 6088	0.166 8113	0.226 6280	0.307 7394	0.252 4963	0.352 5768
112	0.118 5740	0.166 7730	0.226 4931	0.307 5982	0.251 9608	0.352 0192
128	0.118 5514	0.166 7480	0.226 4055	0.307 5066	0.251 6126	0.351 6570
160	0.118 5248	0.166 7187	0.226 3024	0.307 3988	0.251 2025	0.351 2307
192	0.118 5104	0.166 7028	0.226 2464	0.307 3402	0.250 9794	0.350 9989
224	0.118 5017	0.166 6932	0.226 2126	0.307 3049	0.250 8448	0.350 8592
256	0.118 4960	0.166 6870	0.226 1907	0.307 2820	0.250 7573	0.350 7684
384	0.118 4858	0.166 6757	0.226 1509	0.307 2403	0.250 5986	0.350 6036
512	0.118 4822	0.166 6718	0.226 1370	0.307 2258	0.250 5429	0.350 5459
∞	0.118 478	0.166 667	0.226 119	0.307 207	0.250 471	0.350 472

Obviously this modification does not affect the large L behaviour since $A_1^{(0)}(L) = A_1^{(0)}(\infty) + \mathrm{O}(L^{-2})$. It turns out that the results for our largest lattice sizes are virtually unaffected by this kind of improvement.

3.2. Determination of non-universal constants

The matching programme also allows one to determine the non-universal constants appearing in formulae describing the divergence of observables near the roughening transition. In [6] we showed that the two non-universal parameters A and C determining the critical behaviour of the correlation length, (cf equation (17)), can be determined from information of the matching procedure. For one of the models matched with the BCSOS model, one finds

$$A^{\mathrm{SOS}} = b_{\mathrm{m}} A^{\mathrm{BCSOS}} \tag{25}$$

$$C^{\mathrm{SOS}} = q^{-1/2} C^{\mathrm{BCSOS}} \tag{26}$$

where the parameters A^{BCSOS} and C^{BCSOS} can easily be extracted from equation (13). If

$$R = \frac{\partial A_{i,l}^{\mathrm{BCSOS}}}{\partial K^{\mathrm{BCSOS}}} \Big/ \frac{\partial A_{i,l}}{\partial K} \tag{27}$$

where quantities have to be taken at the roughening couplings, is the same for all observables, which is the case for our data, then q is given by

$$q = \frac{K_{\mathrm{R}}^{\mathrm{SOS}}}{K_{\mathrm{R}}^{\mathrm{BCSOS}}} R. \tag{28}$$

For a more detailed discussion see [6].

4. Numerical results

We simulated the BCSOS model at its critical coupling $K_{\mathrm{R}}^{\mathrm{BCSOS}} = \frac{1}{2}\ln 2$ using the loop algorithm of Evertz *et al* [25]. One has to note that periodic boundary conditions of the F-model do not correspond to periodic boundary conditions of the BCSOS model. Therefore updates of loops that wind around the lattice are forbidden.

We performed 10^7 measurements for all lattices sizes considered. We have chosen the number of loop updates between two successive measurements such that the autocorrelation times were about 1.

In addition to the observables $A_{i,l}$ we measured the interface thickness, the total energy E and $A_{i,l} \times E$, which is needed to compute derivatives of the observables with respect to the coupling. In order to save disc space we accumulated 1000 measurements before writing to the file. The statistical errors were computed by jackknifing the 10^4 prebinned data. As random number generator, we used a combination of three shift register generators.

We checked the reliability of the updating program by comparing the estimates from 10^8 measurements for $L = 4$ with the exact results obtained by explicitly averaging over all BCSOS configurations. Our data are also consistent with those of [8]. In [8] lattices of size up to $L = 96$ were used, 4×10^6 measurements were performed, and the G05CAF random number generator of the NAGLIB was used. Note also that the computer programs of [8] were written independently of the programs used in the present study.

The results for the BCSOS observables are summarized in tables 2 and 3. Our estimates for the slopes of the observables are given in tables 4 and 5. With slope we mean the derivative of the observables with respect to the coupling K^{BCSOS}, taken at the critical value.

We then performed the simulations for the ASOS, the DG and the dual of the XY model. The simulations of the ASOS and DG model were performed using a demon version [26] of the Valleys-to-Mountains reflection (VMR) algorithm [27]. The simulation of the dual XY model was performed using the standard version of the VMR algorithm. In both cases we used the G05CAF routine of the NAGLIB as random number generator.

Again we performed 10^7 measurements and accumulated 1000 measurements before writing to the file. In order to obtain estimates for the observables in a neighbourhood of the simulation point, we employed a second-order Taylor expansion (note that the prebinning forbids the use of a reweighting technique). We thus computed the first and second derivatives of the observables,

$$\frac{\mathrm{d}A}{\mathrm{d}K} = \langle H\rangle\langle A\rangle - \langle HA\rangle \tag{29}$$

and

$$\frac{\mathrm{d}^2A}{\mathrm{d}K^2} = \langle H^2A\rangle - 2\langle H\rangle\langle HA\rangle + 2\langle H\rangle^2\langle A\rangle - \langle H^2\rangle\langle A\rangle \tag{30}$$

for the ASOS and the DG model. In the XY case analogous formulae were derived. We carefully checked by comparing with results obtained from simulations at shifted couplings that the Taylor expansion of the $A_{i,l}$ to second order was sufficiently precise.

Table 2. Monte Carlo results for the A_i obtained at the critical coupling of the BCSOS model. The block-observables A_i are defined in the text. L is the original lattice size, and l is the size of the blocked system.

L	l	A_1	A_2	A_3	A_4
16	1			0.265 11(30)	0.067 37(26)
24	1			0.240 04(31)	0.054 37(25)
32	1			0.225 72(32)	0.047 72(25)
40	1			0.215 26(31)	0.043 41(24)
48	1			0.207 78(30)	0.039 59(24)
56	1			0.201 57(31)	0.037 04(24)
64	1			0.196 56(33)	0.035 71(24)
80	1			0.188 84(33)	0.032 52(25)
96	1			0.182 09(34)	0.030 32(25)
112	1			0.177 97(35)	0.028 80(25)
128	1			0.173 99(33)	0.027 50(23)
160	1			0.167 04(37)	0.025 29(26)
192	1			0.163 41(40)	0.024 19(26)
224	1			0.159 35(41)	0.022 65(26)
256	1			0.156 16(42)	0.021 88(26)
16	2	0.085 740(27)	0.117 435(45)	0.223 82(18)	0.055 97(13)
24	2	0.083 135(26)	0.115 240(43)	0.202 29(18)	0.044 36(12)
32	2	0.082 161(25)	0.114 434(42)	0.189 81(19)	0.038 51(12)
40	2	0.081 661(24)	0.113 976(41)	0.180 79(19)	0.034 44(12)
48	2	0.081 351(24)	0.113 660(41)	0.174 09(18)	0.031 74(12)
56	2	0.081 129(24)	0.113 497(41)	0.168 88(19)	0.029 75(12)
64	2	0.080 932(24)	0.113 249(41)	0.164 49(20)	0.028 12(12)
80	2	0.080 719(24)	0.113 064(41)	0.157 67(20)	0.025 67(12)
96	2	0.080 541(24)	0.112 855(41)	0.152 18(21)	0.024 01(12)
112	2	0.080 422(24)	0.112 743(41)	0.148 34(21)	0.022 75(12)
128	2	0.080 306(22)	0.112 617(38)	0.144 85(20)	0.021 45(11)
160	2	0.080 165(25)	0.112 424(42)	0.139 16(23)	0.019 83(12)
192	2	0.080 055(25)	0.112 278(43)	0.135 67(24)	0.018 48(12)
224	2	0.080 008(26)	0.112 258(44)	0.132 25(25)	0.017 63(12)
256	2	0.079 953(26)	0.112 235(45)	0.129 36(26)	0.016 99(13)

We performed the simulations at the previously best known estimates for the roughening couplings [6], namely $K_0^{\mathrm{DG}} = 0.6645$, $K_0^{\mathrm{ASOS}} = 0.8061$, and $\beta_0^{\mathrm{XY}} = 1.1197$.

In order to keep the length of this paper within reasonable bounds, we present the numerical results only for the XY model, see tables 6 and 7. The tables for the other models are available from the authors upon request.

Finally we performed the simulations for the Ising model. The simulations were performed using the VMR algorithm [27] adapted to the Ising interface as discussed in [12, 28].

A number of technical improvements led to a reduction of the CPU time required for a given statistic by a factor of about 4 compared with the code used in [8, 12, 28].

We performed the simulations at the previously best known estimate for the roughening couplings [8], $K_0^1 = 0.407\,54$.

We performed 3×10^6 to 8×10^6 measurements for lattice sizes ranging from $32\times32\times31$ to $192 \times 192 \times 31$. Again we prebinned the results of 1000 measurements before writing to disc.

For the Ising interface we also computed the Taylor expansion of the observables to second order.

Table 3. Continuation of table 2.

L	l	A_1	A_2	A_3	A_4
16	4	0.176 651(27)	0.230 216(40)	0.221 936(80)	0.077 948(65)
24	4	0.165 308(24)	0.219 807(37)	0.194 147(82)	0.052 961(63)
32	4	0.161 166(23)	0.215 927(35)	0.179 384(82)	0.043 583(61)
40	4	0.159 116(22)	0.213 952(35)	0.169 635(82)	0.038 175(60)
48	4	0.157 915(22)	0.212 736(34)	0.162 291(81)	0.034 469(59)
56	4	0.157 067(22)	0.211 902(34)	0.156 869(82)	0.031 988(59)
64	4	0.156 463(21)	0.211 246(34)	0.152 173(85)	0.029 793(59)
80	4	0.155 714(21)	0.210 486(34)	0.145 120(86)	0.026 922(58)
96	4	0.155 185(22)	0.209 912(34)	0.139 701(89)	0.024 779(59)
112	4	0.154 811(21)	0.209 486(34)	0.135 546(90)	0.023 253(58)
128	4	0.154 514(20)	0.209 164(31)	0.131 951(85)	0.021 861(53)
160	4	0.154 099(22)	0.208 674(35)	0.126 456(96)	0.019 967(59)
192	4	0.153 818(22)	0.208 360(35)	0.122 57(10)	0.018 579(58)
224	4	0.153 583(22)	0.208 080(35)	0.119 12(10)	0.017 534(58)
256	4	0.153 391(23)	0.207 869(36)	0.116 47(11)	0.016 720(59)
16	8	0.265 665(22)	0.325 828(30)	0.345 213(51)	1.000 000
24	8	0.216 030(16)	0.280 733(24)	0.227 866(37)	0.105 810(34)
32	8	0.196 646(14)	0.264 669(22)	0.205 656(38)	0.072 017(32)
40	8	0.188 911(14)	0.257 187(21)	0.189 140(37)	0.055 770(31)
48	8	0.184 346(13)	0.252 912(20)	0.179 067(36)	0.048 696(30)
56	8	0.181 606(13)	0.250 139(20)	0.171 361(37)	0.043 493(30)
64	8	0.179 710(13)	0.248 261(20)	0.165 313(38)	0.039 956(30)
80	8	0.177 383(12)	0.245 856(20)	0.156 139(38)	0.034 926(29)
96	8	0.175 951(12)	0.244 337(20)	0.149 442(40)	0.031 601(30)
112	8	0.174 995(12)	0.243 293(20)	0.144 178(39)	0.029 200(29)
128	8	0.174 309(11)	0.242 532(18)	0.139 959(37)	0.027 326(27)
160	8	0.173 355(12)	0.241 458(20)	0.133 345(41)	0.024 585(29)
192	8	0.172 733(12)	0.240 736(20)	0.128 466(43)	0.022 659(29)
224	8	0.172 270(12)	0.240 186(20)	0.124 527(44)	0.021 187(29)
256	8	0.171 898(13)	0.239 742(20)	0.121 338(46)	0.020 028(29)

In the case of the Ising interface we performed, in addition to the matching with the BCSOS model, the matching with the ASOS model at $K_R^{ASOS} = 0.806\,08$, which is our present estimate of the roughening coupling for the ASOS model. For this purpose we performed additional simulations of the ASOS model at $K_R^{ASOS} = 0.806\,08$ for the lattice sizes 24, 48, 56, 80, 112, and 160. The idea behind the matching with the ASOS model is that corrections to scaling in the ASOS model are similar to those of the Ising interface. Therefore it should be possible to obtain reliable estimates for the roughening coupling from smaller lattice sizes this way than from the matching with the BCSOS model.

The total CPU requirement for all our simulations accumulates to nearly 4 years on typical modern workstations. For an overview of the lattice sizes employed and the CPU resources needed for the various models, see table 8.

We extracted all our estimates from the matching of the two observables D_2 and A_3 (the last column in the tables). Here the convergence seems optimal.

To obtain estimates for the roughening couplings and the matching b_m we employed the following

Rule. Start with the largest block lattice size, i.e. $l = 8$ (the statistical errors are the smallest here). As a first estimate E_1 take the value for the largest lattice size L available.

Table 4. Monte Carlo results for the derivatives of the A_i with respect to the coupling, taken for the BCSOS model at the critical coupling. The block observables A_i are defined in the text. L is the original lattice size, and l is the size of the blocked system.

L	l	A_1	A_2	A_3	A_4
16	1			4.9725(59)	2.2881(60)
24	1			5.5222(88)	2.2951(89)
32	1			5.888(12)	2.285(12)
40	1			6.216(14)	2.304(15)
48	1			6.463(17)	2.310(17)
56	1			6.659(20)	2.326(20)
64	1			6.839(23)	2.289(23)
80	1			7.131(29)	2.308(28)
96	1			7.340(34)	2.319(34)
112	1			7.526(40)	2.260(40)
128	1			7.714(42)	2.308(42)
160	1			8.079(59)	2.286(57)
192	1			8.202(71)	2.358(69)
224	1			8.478(81)	2.432(79)
256	1			8.719(95)	2.348(91)
16	2	−0.544 95(72)	−0.7764(12)	3.9804(37)	1.6789(32)
24	2	−0.566 52(96)	−0.8146(16)	4.4235(56)	1.6717(47)
32	2	−0.5876(12)	−0.8476(20)	4.7222(73)	1.6559(59)
40	2	−0.6055(15)	−0.8725(25)	4.9708(89)	1.6655(74)
48	2	−0.6208(17)	−0.8961(29)	5.172(11)	1.6574(88)
56	2	−0.6331(20)	−0.9126(34)	5.345(13)	1.659(10)
64	2	−0.6469(23)	−0.9316(38)	5.484(14)	1.642(12)
80	2	−0.6644(28)	−0.9587(47)	5.744(18)	1.651(14)
96	2	−0.6806(33)	−0.9807(56)	5.907(21)	1.620(17)
112	2	−0.6822(39)	−0.9882(67)	6.056(25)	1.659(20)
128	2	−0.7079(40)	−1.0227(68)	6.189(26)	1.639(21)
160	2	−0.7199(55)	−1.0320(94)	6.474(36)	1.641(29)
192	2	−0.7412(64)	−1.072(11)	6.571(44)	1.642(35)
224	2	−0.7613(75)	−1.103(13)	6.734(50)	1.655(40)
256	2	−0.7748(88)	−1.121(15)	6.939(58)	1.592(46)

Then check whether the estimate is 2σ-compatible with the results (also for $l = 8$) for the next two smaller lattice sizes. 2σ-compatibility of two estimates m_1, m_2 with statistical errors e_1, e_2 here means that $|m_1 - m_2| < 2\,[e_1^2 + e_2^2]^{1/2}$. Then also check the 2σ-consistency of E_1 with the estimates for the three largest available L values for $l = 4$ and $l = 2$. If the estimates are consistent, take E_1 as the final estimate. Otherwise restart the whole procedure with $l = 4$, i.e. take as the first estimate E_1 the value from the largest L and $l = 4$. If there is again a failure, restart at $l = 2$.

Given that the corrections die out like L^{-2} our rule ensures that systematic errors in the determination of the roughening coupling are smaller than the statistical errors quoted.

We invite the careful reader to go through this procedure in the case of the XY model (tables 6 and 7). Our final estimates for the critical couplings and the matching b_{m}, together with the values of l and L where the decision procedure stopped, are given in table 9.

In order to determine the non-universal constants A and C we need estimates for the ratios of slopes R defined in equation (27). These ratios for the different observables and for the different block/lattice sizes are presented (for the XY model as an example) in table 10. From this table, and from the corresponding tables for the other SOS models and the Ising

Table 5. Continuation of table 4.

L	l	A_1	A_2	A_3	A_4
16	4	−1.024 43(81)	−1.3944(12)	2.9483(20)	1.5854(17)
24	4	−1.0343(10)	−1.4308(15)	3.2837(29)	1.4291(24)
32	4	−1.0626(12)	−1.4790(18)	3.5337(36)	1.3832(30)
40	4	−1.0909(14)	−1.5208(22)	3.7292(44)	1.3796(37)
48	4	−1.1165(17)	−1.5573(26)	3.8885(51)	1.3631(44)
56	4	−1.1395(19)	−1.5901(30)	4.0296(61)	1.3619(51)
64	4	−1.1596(21)	−1.6176(33)	4.1442(67)	1.3456(58)
80	4	−1.1943(26)	−1.6676(41)	4.3474(85)	1.3524(72)
96	4	−1.2182(31)	−1.7022(48)	4.491(10)	1.3459(87)
112	4	−1.2410(36)	−1.7339(56)	4.627(12)	1.3395(99)
128	4	−1.2668(37)	−1.7680(58)	4.744(12)	1.329(10)
160	4	−1.2935(50)	−1.7997(78)	4.942(17)	1.361(14)
192	4	−1.3372(59)	−1.8660(92)	5.055(20)	1.372(17)
224	4	−1.3603(68)	−1.897(11)	5.186(23)	1.352(20)
256	4	−1.3771(79)	−1.921(12)	5.351(27)	1.330(23)
16	8	−1.272 54(71)	−1.652 59(97)	2.6102(15)	0.000 00
24	8	−1.095 26(73)	−1.5480(11)	2.4655(15)	1.4653(13)
32	8	−1.099 68(81)	−1.5481(12)	2.7517(19)	1.4710(16)
40	8	−1.103 06(92)	−1.5727(14)	2.9006(22)	1.3380(19)
48	8	−1.1188(10)	−1.6001(16)	3.0496(26)	1.3139(22)
56	8	−1.1344(12)	−1.6265(18)	3.1721(30)	1.2878(26)
64	8	−1.1514(13)	−1.6537(20)	3.2715(34)	1.2758(30)
80	8	−1.1828(16)	−1.7011(25)	3.4528(41)	1.2607(36)
96	8	−1.2067(18)	−1.7356(29)	3.5904(50)	1.2524(43)
112	8	−1.2338(21)	−1.7768(33)	3.7300(58)	1.2482(50)
128	8	−1.2553(21)	−1.8070(34)	3.8241(59)	1.2377(52)
160	8	−1.2906(29)	−1.8574(46)	4.0041(81)	1.2439(71)
192	8	−1.3261(34)	−1.9101(54)	4.1256(99)	1.2387(85)
224	8	−1.3503(39)	−1.9428(62)	4.252(11)	1.240(10)
256	8	−1.3741(45)	−1.9792(72)	4.382(13)	1.230(11)

model, we extracted by applying again our rule a final estimate for the ratio of slopes R. Our estimates for the non-universal constants A and C are given in table 11.

5. Comparison with previous studies

In this section we present a comparison of our present results with some previous estimates on the critical couplings $K_{\rm R}$ and non-universal parameters A and C.

Let us start with the DG model. See table 12 for two estimates from the 1970s and some more modern results that can be compared with the present estimates. A comparison of the findings in [31] and [32] with the estimates of [6] was presented in [6]. We would just like to comment at the apparent 1σ-incompatibility of the present estimate for $K_{\rm R}^{\rm DG}$ with that of [6]. A closer look at our data reveals that this is most likely a statistical fluctuation: discarding the $L = 48$ and $L = 64$ lattices from the analysis does not move our present estimate towards the result in [6], which was obtained with the same method and with lattices of size up to $L = 32$.

We now turn to the XY model. A table of previous estimates in comparison with previously published results is given in table 13. We find our present estimates consistent

Table 6. XY results for the matching factor obtained in the way described after equation (22).

L	l	A_1, A_3	A_2, A_3	D_1, A_3	D_2, A_3
32	2	0.9176(46)	0.9381(65)	0.9007(55)	0.9273(74)
48	2	0.9239(62)	0.9307(78)	0.9148(69)	0.9235(86)
64	2	0.9206(80)	0.9275(92)	0.9148(86)	0.9231(97)
96	2	0.9362(97)	0.9386(117)	0.9335(101)	0.9365(121)
128	2	0.9376(107)	0.9356(118)	0.9362(109)	0.9345(120)
192	2	0.9275(136)	0.9331(170)	0.9266(138)	0.9324(172)
32	4	0.8896(14)	0.9035(17)	0.8601(18)	0.8820(20)
48	4	0.9080(20)	0.9162(23)	0.8923(24)	0.9045(26)
64	4	0.9172(27)	0.9231(31)	0.9082(29)	0.9165(33)
96	4	0.9263(36)	0.9300(38)	0.9217(38)	0.9266(40)
128	4	0.9364(40)	0.9363(43)	0.9340(41)	0.9345(45)
192	4	0.9287(50)	0.9271(52)	0.9273(51)	0.9260(52)
32	8	0.8421(3)	0.8622(4)	0.7731(6)	0.8149(6)
48	8	0.8760(6)	0.8903(7)	0.8329(8)	0.8610(9)
64	8	0.8890(8)	0.9009(10)	0.8629(10)	0.8825(11)
96	8	0.9118(11)	0.9199(13)	0.8988(13)	0.9109(14)
128	8	0.9185(14)	0.9245(16)	0.9109(16)	0.9191(17)
192	8	0.9267(19)	0.9297(21)	0.9227(20)	0.9269(22)

Table 7. XY results for the roughening coupling obtained in the way described after equation (22).

L	l	A_1, A_3	A_2, A_3	D_1, A_3	D_2, A_3
32	2	1.119 982(94)	1.119 545(117)	1.120 352(105)	1.119 773(133)
48	2	1.119 933(90)	1.119 822(120)	1.120 084(98)	1.119 940(130)
64	2	1.119 757(95)	1.119 661(114)	1.119 839(100)	1.119 722(119)
96	2	1.119 707(86)	1.119 682(101)	1.119 735(89)	1.119 703(104)
128	2	1.119 831(92)	1.119 852(102)	1.119 845(94)	1.119 863(104)
192	2	1.119 789(92)	1.119 742(114)	1.119 797(93)	1.119 748(115)
32	4	1.120 176(48)	1.119 726(53)	1.121 162(52)	1.120 428(59)
48	4	1.120 034(46)	1.119 846(51)	1.120 403(50)	1.120 116(55)
64	4	1.119 868(45)	1.119 754(52)	1.120 044(47)	1.119 883(55)
96	4	1.119 791(41)	1.119 735(49)	1.119 860(42)	1.119 785(51)
128	4	1.119 798(41)	1.119 800(48)	1.119 829(42)	1.119 823(48)
192	4	1.119 866(42)	1.119 884(47)	1.119 881(43)	1.119 896(48)
32	8	1.120 078(32)	1.118 559(33)	1.125 145(34)	1.122 223(39)
48	8	1.120 069(29)	1.119 442(29)	1.121 941(28)	1.120 741(33)
64	8	1.120 095(26)	1.119 701(28)	1.120 979(28)	1.120 310(30)
96	8	1.119 951(26)	1.119 754(26)	1.120 271(26)	1.119 973(27)
128	8	1.119 906(24)	1.119 789(26)	1.120 057(25)	1.119 894(27)
192	8	1.119 888(22)	1.119 841(24)	1.119 949(23)	1.119 885(24)

with our previous results in [6]. In figure 1 we have plotted the estimates for the XY transition coupling given in table 13. The two horizontal lines give the 1σ error range of our present estimate.

Table 8. The lattice sizes L employed in our simulations of the various models, together with the CPU resources needed on an 'average modern workstation'.

Model	Lattice sizes	CPU
BCSOS	16, 24, 32, 40, 48, 56, 64, 80, 96, 112, 128, 160, 192, 224, 256	200 d
XY	32, 48, 64, 96, 192	70 d
ASOS	32, 48, 64, 96, 128, 192, 256, 384, 512	440 d
DG	16, 24, 32, 48, 64	15 d
Ising	32, 48, 64, 96, 128, 192	650 d

Table 9. Our results for the roughening couplings and the matching b_m, together with the l, L values that were used (see rule). In the Ising model case, the index 'a' refers to the matching with the BCSOS model, the index 'b' refers to the matching with the ASOS model.

model	K_R	From l, L	b_m	From l, L
XY	1.1199(1)	4, 192	0.93(1)	4, 192
ASOS	0.806 08(2)	8, 512	2.78(3)	4, 512
DG	0.6653(2)	2, 64	0.32(1)	2, 64
Ising a	0.407 59(2)	2, 192	3.20(4)	2, 192
Ising b	0.407 58(1)	8, 192	3.21(3)	8, 192

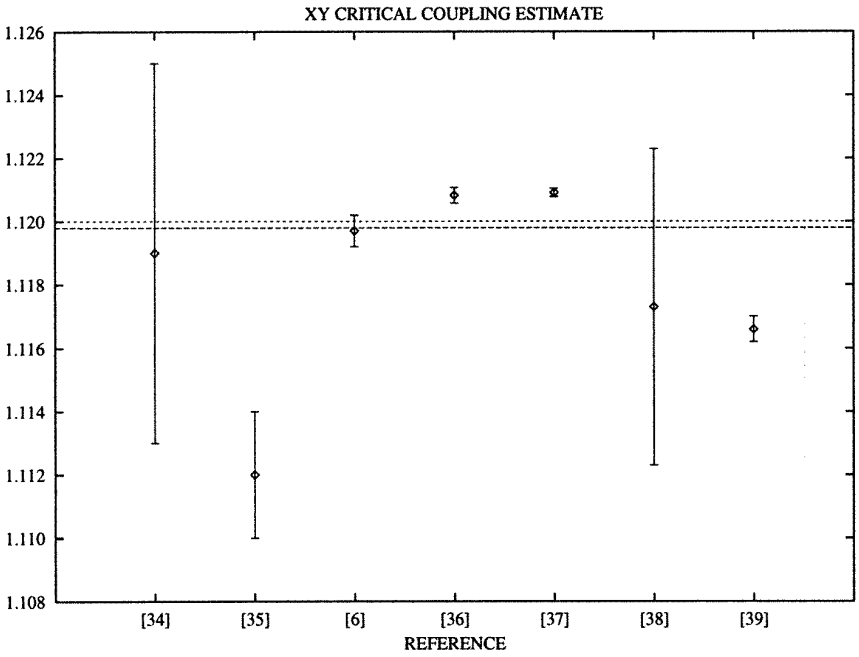

Figure 1. The results for the critical coupling of the two-dimensional XY model as listed in table 13. The corresponding references to the literature are given (in square brackets) as labels of the x-axis. The two horizontal lines give the error range of the result of the present work.

Most of the results of the other authors, also the estimates from series analysis by Campostrini *et al* [39] are inconsistent with the present estimate. We conclude that in all these cases the systematic errors due to corrections to scaling are underestimated.

Table 10. Monte Carlo estimates for the ratio of slopes for the XY and BCSOS model block observables, taken at the critical couplings, cf the definition in equation (27).

L	l	D_1	D_2	A_1	A_2
16	1			−0.4167(14)	−0.4137(17)
24	1			−0.4206(14)	−0.4195(25)
32	1			−0.4249(17)	−0.4227(33)
48	1			−0.4252(19)	−0.4267(48)
64	1			−0.4255(24)	−0.4270(67)
96	1			−0.4257(32)	−0.4410(99)
128	1			−0.4267(41)	−0.439(13)
192	1			−0.4280(59)	−0.413(19)
16	2	−0.4271(11)	−0.4302(11)	−0.4154(13)	−0.4046(12)
24	2	−0.4299(13)	−0.4314(13)	−0.4194(13)	−0.4112(17)
32	2	−0.4298(15)	−0.4304(14)	−0.4236(14)	−0.4167(23)
48	2	−0.4288(19)	−0.4285(19)	−0.4244(17)	−0.4195(34)
64	2	−0.4281(23)	−0.4285(24)	−0.4238(20)	−0.4271(46)
96	2	−0.4355(33)	−0.4365(33)	−0.4263(25)	−0.4326(70)
128	2	−0.4250(41)	−0.4252(42)	−0.4281(32)	−0.4140(92)
192	2	−0.4282(60)	−0.4277(62)	−0.4276(46)	−0.412(14)
16	4	−0.419 61(73)	−0.425 05(77)	−0.4070(13)	−0.3657(12)
24	4	−0.425 92(89)	−0.428 39(90)	−0.4140(13)	−0.3962(11)
32	4	−0.429 65(98)	−0.430 38(95)	−0.4182(13)	−0.4061(14)
48	4	−0.4290(12)	−0.4291(11)	−0.4218(13)	−0.4148(21)
64	4	−0.4294(13)	−0.4296(13)	−0.4213(15)	−0.4187(28)
96	4	−0.4324(17)	−0.4323(17)	−0.4250(17)	−0.4236(43)
128	4	−0.4296(21)	−0.4290(20)	−0.4264(21)	−0.4177(57)
192	4	−0.4295(30)	−0.4300(29)	−0.4281(29)	−0.4050(85)
24	8	−0.422 39(92)	−0.423 00(69)	−0.4120(18)	−0.383 03(53)
32	8	−0.423 73(70)	−0.427 91(81)	−0.4087(11)	−0.3694(18)
48	8	−0.428 71(87)	−0.430 10(86)	−0.4147(13)	−0.3952(12)
64	8	−0.429 60(99)	−0.430 30(95)	−0.4177(13)	−0.4035(15)
96	8	−0.4320(12)	−0.4328(12)	−0.4204(15)	−0.4159(23)
128	8	−0.4313(14)	−0.4311(13)	−0.4228(15)	−0.4192(31)
192	8	−0.4311(18)	−0.4307(17)	−0.4267(19)	−0.4175(48)

Table 11. Our results for the non-universal constants A and C. In the Ising model case, the index 'a' refers to the matching with the BCSOS model, the index 'b' refers to the matching with the ASOS model.

Model	A	C
XY	0.233(3)	1.776(4)
ASOS	0.695(8)	1.099(4)
DG	0.080(3)	2.438(6)
Ising a	0.80(1)	1.03(2)
Ising b	0.80(1)	1.01(1)

In the case of the ASOS model, see table 14, we only compare with our previous estimate [6] and with an estimate by Adler from a ninth-order low-temperature series. The series estimate has a quite large error, but is consistent with our result.

Table 12. Comparison of our results for the DG model with previous estimates.

Authors	Year	K_R^{DG}	A	C
Swendsen [29]	1977	0.77(6)		
Shugard *et al* [30]	1978	0.68		
Janke and Nather [31]	1991	0.665(5)		
fit 1		0.6657(3)	0.1204(18)	2.370(11)
fit 2		0.6595(3)	0.0287(7)	2.812(14)
Evertz *et al* [32]	1993	0.662(3)		
Hasenbusch *et al* [7, 6]	1992/94	0.6645(6)	0.078(5)	2.44(3)
Hasenbusch and Pinn, this work	1996	0.6653(2)	0.080(3)	2.438(6)

Table 13. Comparison of our results for the XY model with previous estimates.

Authors	Year	K_R^{XY}	A	C
Baillie and Gupta [33]	1991	1.1218	0.2129	1.7258
Baillie and Gupta [34]	1992	1.119(6)		
Biferale [35]	1989	1.112(2)		1.74(20)
Hasenbusch *et al* [6]	1992/94	1.1197(5)	0.223(13)	1.78(2)
Olsson [36]	1994	1.120 82(25)		1.585(9)
Olsson [37]	1995	1.120 91(13)		1.59(2)
Schultka and Manousakis [38]	1994	1.1173(50)		1.800(2)
Campostrini *et al* [39]	1996	1.1166(4)		
Hasenbusch and Pinn, this work	1996	1.1199(1)	0.233(3)	1.776(4)

Table 14. Comparison of our results for the ASOS model with previous estimates.

Authors	Year	K_R^{ASOS}	A	C
Shugard *et al* [30]	1978	0.81		
Adler [40]	1987	0.787(24)		
Hasenbusch *et al* [7, 6]	1992/94	0.8061(3)	0.70(8)	1.14(2)
Hasenbusch and Pinn, this work	1996	0.806 08(2)	0.695(8)	1.099(4)

We conclude this section with a comparison of the Ising interface estimates, see table 15. Here we find that all the cited estimates of the roughening couplings are consistent with each other. Note, however, the large errors in the estimates that were obtained with techniques other than the matching method. The estimate of Mon *et al* [41] for A seems to be the result of a wrong method.

6. Conclusions and outlook

By increasing the statistics by a factor of about 100 and by also using larger lattices compared to [6], we obtained the most accurate estimates for the roughening couplings of the Ising interface, the ASOS model, the DG model and the 2D XY model published so far. In contrast to other methods, systematical errors are under control. We believe that the strong discrepancies in the estimates of the XY critical coupling of other authors with our results are due to neglection or incomplete handling of the corrections to scaling.

Table 15. Comparison of our results for the Ising model with previous estimates. The index 'a' refers to matching with the BCSOS model, whereas the 'b' means matching with the ASOS model.

Authors	Year	K_R^I	A	C
Weeks *et al* [10]	1973	0.39		
Bürkner and Stauffer [11]	1983	0.396(22)		
Adler [40]	1987	0.404(12)		
Mon *et al* [41]	1988	0.410(16)	9.8(2.0)	1.36(6)
Mon *et al* [42]	1990	0.409(4)		
Hasenbusch [7]	1992	0.4074(3)		
Hasenbusch *et al* [8]	1996	0.407 54(5)	0.74(2)	1.03(2)
Hasenbusch and Pinn, this work, a	1996	0.407 59(2)	0.80(1)	1.03(2)
Hasenbusch and Pinn, this work, b	1996	0.407 58(1)	0.80(1)	1.01(1)

The matching procedure converges like L^{-2} while other methods that rely on analytic results derived from KT theory are plagued by corrections logarithmic in the lattice size. In addition to the precise numbers for the roughening coupling and other non-universal constants the matching provides an unambigous confirmation of the KT nature of the phase transition of the models considered. It is interesting to compute the observables used for the matching method for the sine–Gordon model in perturbation theory. This will allow one to rederive the KT flow equations from finite size scaling. Furthermore, it will provide quantitative information about the RG flow, in particular about the critical trajectory, which can be compared with the numerical results given in the present paper.

Acknowledgments

A large part of the simulations have been performed on the SR2001 of Hitachi Europe, Ltd. The remaining part of the simulations was done on workstations of the Institut für Numerische und Instrumentelle Mathematik der Universität Münster and of the DAMTP, Cambridge University. This work was supported by the Leverhulme Trust under grant 16634-AOZ-R8 and by PPARC.

References

[1] To give only a few references:
Kosterlitz J M and Thouless D J 1973 *J. Phys. C: Solid State Phys.* **6** 1181
Kosterlitz J M 1974 *J. Phys. C: Solid State Phys.* **7** 1046
Chui S T and Weeks J D 1976 *Phys. Rev.* B **14** 4978
José J V, Kadanoff L P, Kirkpatrick S and Nelson D R 1977 *Phys. Rev.* B **16** 1217
Ohta T and Kawasaki K 1978 *Prog. Theor. Phys.* **60** 365
Amit D J, Goldschmidt Y Y and Grinstein G 1980 *J. Phys. A: Math. Gen.* **13** 585
[2] van Beijeren H 1977 *Phys. Rev. Lett.* **38** 993
[3] Lieb E H 1967 *Phys. Rev.* **162** 162
[4] Lieb E H and Wu F Y 1972 *Phase Transitions and Critical Phenomena* vol 1, ed C Domb and N S Green (New York: Academic)
[5] Baxter R J 1982 *Exactly Solved Models in Statistical Mechanics* (New York: Academic)
[6] Hasenbusch M, Marcu M and Pinn K 1994 *Physica* **208A** 124
[7] Hasenbusch M 1992 *PhD Thesis* Universität Kaiserslautern
[8] Hasenbusch M, Meyer S and Pütz M 1996 *J. Stat. Phys.* **85** 383
[9] Blöte H W J, Luijten E and Heringa J R 1995 *J. Phys. A: Math. Gen.* **28** 6289
[10] Weeks J D, Gilmer G H and Leamy H J 1973 *Phys. Rev. Lett.* **31** 549

[11] Bürkner E and Stauffer D 1983 *Z. Phys.* B **53** 241
[12] Hasenbusch M and Pinn K 1993 *Physica* **192A** 342
[13] Abraham D B 1986 *Phase Transitions and Critical Phenomena* vol 10, ed C Domb and J L Lebowitz (New York: Academic)
[14] van Beijeren H and Nolden I 1987 *Structure and Dynamics of Surfaces II (Topics in Current Physics 43)* ed W Schommers and P van Blanckenhagen (New York: Springer)
[15] Forgacs G, Lipowsky R and Nieuwenhuizen Th M 1991 *Phase Transitions and Critical Phenomena* vol 14, ed C Domb and J L Lebowitz (New York: Academic)
[16] Gallet F, Balibar S and Rolley E 1987 *J. Physique* **48** 353, 369
Robinson I K, Vlieg E, Hornis H and Conrad E H 1991 *Phys. Rev. Lett.* **67** 1890
Häkkinen H, Merikoski J, Manninen M, Timonen J and Kaski K 1993 *Phys. Rev. Lett.* **70** 2451
[17] Savit R 1980 *Rev. Mod. Phys.* **52** 453 and references therein
[18] Yamamoto H 1979 *Prog. Theor. Phys.* **61** 363
Samuel S 1978 *Phys. Rev.* D **18** 1916
Swendsen R H 1978 *Phys. Rev.* B **17** 3710
Nienhuis B 1984 *J. Stat. Phys.* **34** 731
[19] Nolden I 1990 Equilibrium crystal shapes *PhD Thesis* Utrecht
[20] Itzykson C and Drouffe J M 1989 *Statistical Field Theory* (Cambridge: Cambridge University Press)
[21] Nightingale M P 1976 *Physica* **83A** 561
[22] Binder K 1981 *Z. Phys.* B **43** 119
[23] Kadanoff L P 1966 *Physics* **2** 263
[24] Wilson K G 1974 *Physica* **73** 119
Wilson K G and Kogut J 1974 *Phys. Rep.* C **12** 75 and references therein
[25] Evertz H G, Marcu M and Lana G 1993 *Phys. Rev. Lett.* **70** 875
[26] Creutz M 1983 *Phys. Rev. Lett.* **50** 1411
[27] Evertz H G, Hasenbusch M, Marcu M, Pinn K and Solomon S 1991 *Phys. Lett.* **254B** 185
[28] Hasenbusch M and Meyer S 1991 *Phys. Rev. Lett.* **66** 530
[29] Swendsen R H 1977 *Phys. Rev.* B **15** 5421
[30] Shugard W J, Weeks J D and Gilmer G H 1978 *Phys. Rev. Lett.* **41** 1399
[31] Janke W and Nather K 1991 *Phys. Lett.* **157A** 11
[32] Evertz H G, Hasenbusch M, Marcu M and Pinn K 1993 *Physica* **199A** 31
[33] Baillie C F and Gupta R 1991 *Nucl. Phys.* B (Proc. Suppl.) **20** 669
[34] Baillie C F and Gupta R 1992 *Phys. Rev.* B **45** 2883
[35] Biferale L and Petronzio R 1989 *Nucl. Phys.* B **328** 677
[36] Olsson P 1994 *Phys. Rev. Lett.* **73** 3339
[37] Olsson P 1995 *Phys. Rev.* B **52** 4526
[38] Schultka N and Manousakis E 1994 *Phys. Rev.* B **49** 12 071
[39] Campostrini M, Pelisetto A, Rossi P and Vicari E 1996 *Phys. Rev.* B **54** 7301
[40] Adler J 1987 *Phys. Rev.* B **36** 2473
[41] Mon K K, Wansleben S, Landau D P and Binder K 1988 *Phys. Rev. Lett.* **60** 708
[42] Mon K K, Landau D P and Stauffer D 1990 *Phys. Rev.* B **42** 545